

# OPTIMIZATION OF OPTICS AT 200 MEV KEK-ERL TEST FACILITY FOR SUPPRESSION OF EMITTANCE GROWTH INDUCED BY CSR

M. Shimada\*, A. Enomoto, T. Suwada, K. Yokoya, KEK, Tsukuba, Japan

## Abstract

Energy Recovery Linac (ERL) gets a lot of attention as a next period light source instrument. To produce high-brightness and short pulse synchrotron lights, it is necessary to pass through high current and short bunch electron beams to the insertion part of ERL with keeping the low emittance and the low energy spread. However, it is challenging because Coherent Synchrotron Radiation (CSR) generated at dipole magnets is potential source of the emittance growth which is enormous especially for high current, short bunch and a low energy beam. Therefore, 0.1 psec short bunch beam is accomplished by a gradual bunch compression in the arc after accelerating the beam up to the full energy. The beam optics and lattice design of the first scheme 200 MeV KEK-ERL test facility, which is based on the previous design parameters, is optimized to suppress the emittance growth caused by CSR at the arc section under the twice of the initial emittance.

## INTRODUCTION

To produce high quality synchrotron lights, it is necessary to transport high-current and short-bunch electron beams with keeping emittance and energy spread lower. Energy Recovery Linac (ERL) is expected to produce such a high quality electron beam, therefore, KEK has been planned a KEK-ERL test facility with an energy of 200 MeV as a first step for 5 GeV KEK-ERL. Here, we introduced the first scheme of KEK-ERL test facility [1]. One of the main R&D program is to establish a compensation scheme of the emittance growth caused by CSR. Here, we optimized the lattice design and beam optics of the arc section satisfying requirement that the emittance growth factor is less than twice at the insertion devices.

## LATTICE OPTIMIZATION IN THE ARC SECTION

### Coherent synchrotron radiation and emittance growth mechanism

CSR emitted from a bended electron beam induces an energy dispersion along the bunch [2]. For a gaussian bunch, the change in the energy distribution is followed by,

$$\Delta E \propto -I(\rho^2 \sigma_z^4)^{-1/3}, \quad (1)$$

where  $\sigma_z$ ,  $\rho$  and  $I$  is the rms bunch length, the curvature radius of the dipole magnet and the bunch current, respectively. According to Eq.1, it is clear that the change in

\*Present Affiliation: UVSOR, Institute of Molecular Science, Okazaki, Japan, shimada@ims.ac.jp

bunch energy is larger for the electron beam with a shorter bunch and higher current.

### Minimization of emittance growth induced by CSR

By energy change along the bunch induced by CSR in dipole magnets, the emittance growth does not recover even after an achromatic cell because of aberration from the nominal orbit. Therefore, the coordinates  $(x, x')$  of the particles with the chromatic aberration are shifted on the transverse phase space toward  $\Delta x/\Delta x' = \sin \phi/\rho(1 - \cos \phi)$ , where  $\phi$  is the bending angle of the dipole magnet.

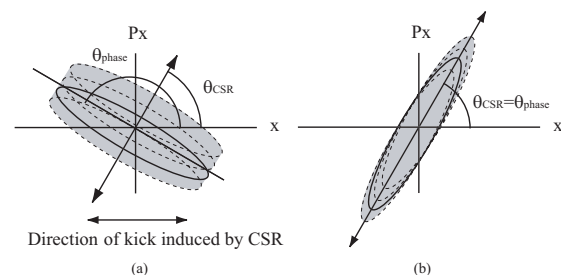


Figure 1: Relationship between the kick direction of CSR,  $\theta_{CSR}$ , and the long axes of the transverse phase spaces,  $\theta_{phase}$ . The emittance growth is minimized when the two angles match each other. Emittance growth is (a): large, and (b): small

The motion of sliced bunches in the transverse phase space after the dipole magnet shown in Fig.1 indicates that the emittance growth is minimized if the kick angle of CSR ( $\theta_{CSR}$ ) is equal to the angle of the long axis of the ellipse phase space ( $\theta_{phase}$ ) at the end of the dipole magnet [3]. The angle  $\theta_{phase}$  can be estimated by using the following formula,  $\tan 2\theta_{phase} = 2\alpha/(\gamma - \beta)$ , where  $\alpha$ ,  $\beta$  and  $\gamma$  are the Twiss parameters [4].

## SIMULATION STUDY OF THE BUNCH COMPRESSION OPTIMIZATION

### A layout and parameters of KEK-ERL test facility

A layout of the KEK-ERL test facility is shown in Fig. 2 and main parameters are summarized in Table.1. An electron beam with a normalized emittance of 100 nm-rad is generated from an electron gun with a laser-photo cathode and merged to the main superconducting linear accelerator with a chicane. In the main linac, the electron beam is accelerated up to about 200 MeV by the superconducting

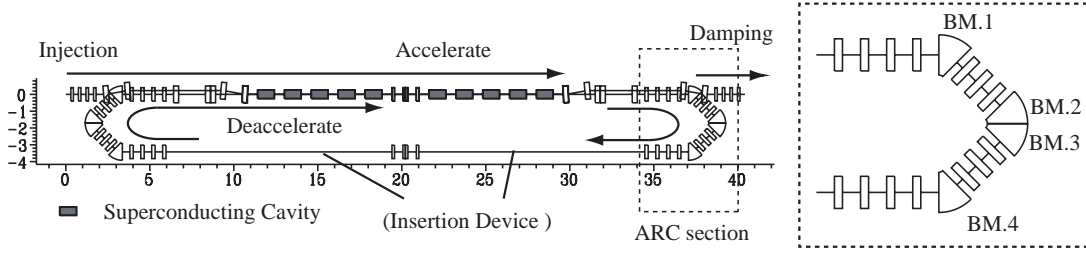


Figure 2: Lattice geometry of the KEK-ERL test facility

Table 1: Main parameters of the KEK-ERL test facility

Main parameter	Design value
Injection beam energy	5 MeV
Maximum beam energy	205 MeV
Operating frequency	1.3 GHz
RF cavity gradient	20 MV/m
Initial normalized emittance	100 nm-rad
Initial rms bunch length	1 psec
Final rms bunch length	0.1 psec
Initial rms energy spread	$5 \times 10^{-5}$
Total length	117.98 m

rf cavities which are similar to TESLA cavities [5]. The arc section composes a triple-bend achromat (TBA) lattice including four dipole magnets and insertion devices are installed after the arc section.

### Optics in arc section and tracking simulation

The bunch length is compressed at the non-zero  $R_{56}$  arc section,  $\Delta z \cong R_{56} \Delta E / E_0$  where  $z$  is relative longitudinal position in canonical axis, after accelerated by off-crest rf phase. The bunch compression is performed after the full acceleration because the emittance of the bunch is easily increased due to CSR in the low energy region such as the merger section.  $R_{56}$  of the present arc design is variable from zero to -0.6 without any influence upon the other beam optics. In the designed arc sections, we controlled the rf phase and the initial energy spread to satisfy the requirement that  $\sigma_z < 0.1$  psec and the emittance,  $\varepsilon_x < 200$  nm-rad at the insertion device.

## RESULT

At first, we tried to match  $\theta_{\text{phase}}$  at the fourth dipole magnet with  $\theta_{\text{CSR}}$ . Figure 3 shows  $\theta_{\text{phase}}$  as a function of  $R_{56}$ . In the gray zone in which  $R_{56} > -0.2$ , the phase space loses the ellipse shape due to the higher order of the large energy spread,  $\Delta E / E_0$ , and it results in a significant growth of the normalized emittance. According to Fig.3, the angle  $\theta_{\text{phase}}$  is close to  $\theta_{\text{CSR}}$  around  $R_{56} = -0.5$ . Therefore, the arc section in the condition that  $R_{56} = -0.5$

is optimal optics from the view of the accordance between the angles.

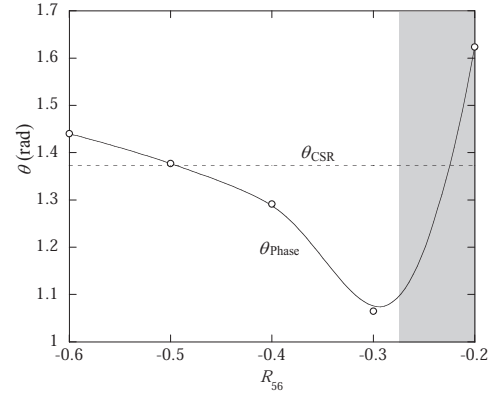


Figure 3: Phase space angles  $\theta_{\text{phase}}$  at the end of the fourth dipole magnet are calculated by the Twiss parameters ( $\circ$ ) and direction in CSR kick,  $\theta_{\text{CSR}}$ , estimated by the curvature radius and bending angle of the dipole magnets (dotted line). In the gray zone, the phase space loses the ellipse shape because of large energy spread.

Figure 5 shows tracking data of the longitudinal phase space and the histogram of the bunch distribution along the longitudinal axis at the insertion device with  $R_{56}$  of -0.3, -0.45 and -0.6. When  $R_{56}$  is larger negative value, the bunch head is sharper by the CSR effect, which is a source of the strong CSR inducing the significant emittance growth. From the view of the CSR effect,  $R_{56}$  with smaller negative value is better to reduce the CSR effects.

Next, the tracking simulation results of the transverse emittance growths are shown in Fig.5. When  $R_{56} = -0.3$ , the emittance growth is large because of the mismatch of the  $\theta_{\text{phase}}$  with  $\theta_{\text{CSR}}$ . On the other hand, in the case that  $R_{56} = -0.6$ , the shift on the transverse phase space is large because of the strong CSR kick.

Finally, the optimum design of the arc section in KEK-ERL test facility is discussed. In the condition that  $\varepsilon_x < 200$  nm-rad and  $\sigma_z < 0.1$  psec at the insertion device, the maximum allowable current reached at 30 mA when  $R_{56} = -0.45$  as shown in Fig.6. The energy spread at the insertion device  $\sigma_{E_f} / E_0$  is  $8.6 \times 10^{-4}$  at the optimum optics.

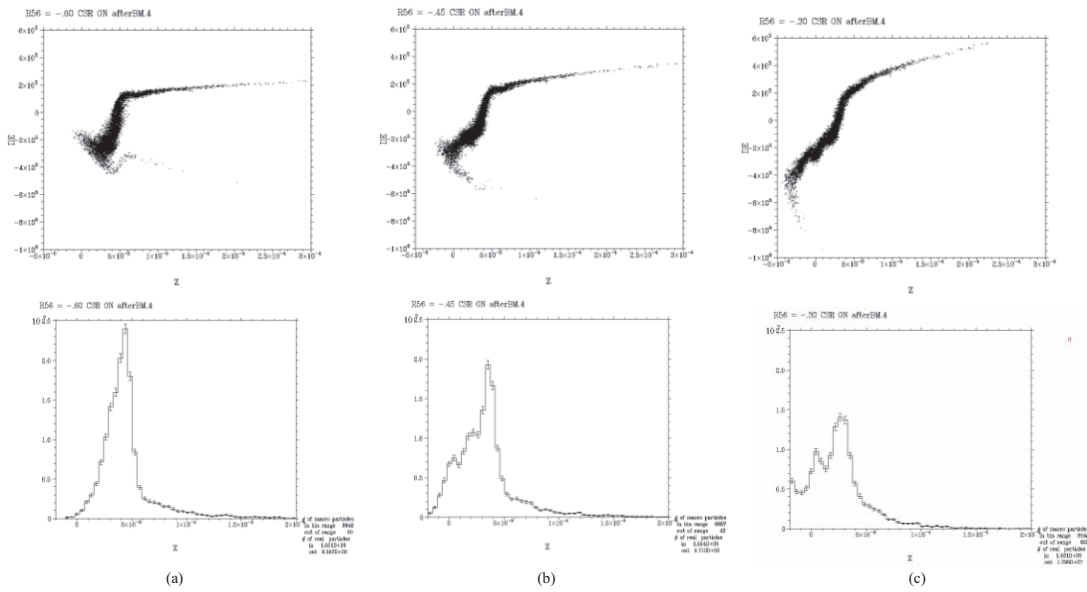


Figure 4: Longitudinal phase space distortion due to CSR and the histograms where  $R_{56}$  is -0.6 (a), -0.45 (b), -0.3 (c), respectively

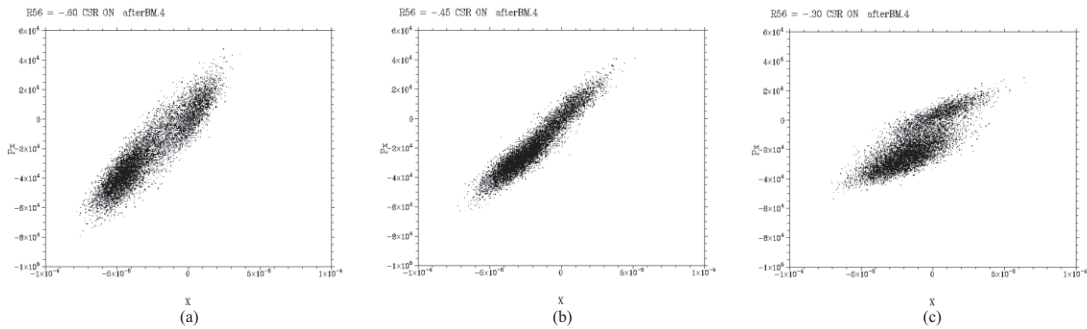


Figure 5: Transverse emittance growth due to CSR where  $R_{56}$  is -0.6 (a), -0.45 (b), -0.3 (c), respectively

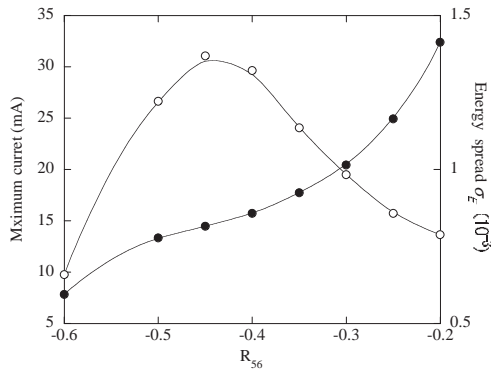


Figure 6: Maximum current ( $\circ$ ) and final energy spread  $\sigma_{E_f}/E_0$  ( $\bullet$ ) under the condition that  $\epsilon_x < 200$  nm-rad and  $\sigma_z < 0.1$  psec at the insertion devices.

**CONCLUSION**

To minimize the emittance growth, the direction of CSR,  $\theta_{CSR}$ , should correspond to the phase space angle,  $\theta_{phase}$ ,

which depends on  $R_{56}$  at the arc section. On the other hand, the emittance growth due to CSR is larger when the values of  $R_{56}$  is larger negative value. In the case of the KEK-ERL test facility, the maximum allowable current achieves 30 mA with keeping less than twice of the initial emittance in the optimum lattice design of the arc section and the beam optics.

**REFERENCES**

- [1] E. Kim and K. Yokoya, Proceedings of the APAC2004, Gyeongju, Korea, 2004, pp.22-26.
- [2] Y. S. Derbenev et al, TESLA-FEL 95-05, (1995) ; T. Agoh, Doctoral thesis, University of Tokyo, (2004).
- [3] R. Hajima, Nucl. Instr. and Meth. A528 (2004) 335.
- [4] H. Wiedemann, Particle Accelerator Physics I 2nd Edit., springer, NewYork, 1999, p.152.
- [5] R. Brinkmann et al (Eds.), TESLA Technical Design Report Part II, (2001).